Int. J. Heat Mass Transfer. Vol. 34, No. 4/5, pp. 1281–1291, 1991
Printed in Great Britain

0017–9310/91 $3.00+0.00
Pergamon Press plc

The effects of inlet conditions on mass transfer in annular swirling decaying flow

P. LEGENTILHOMME and J. LEGRAND†
Laboratoire de Génie des Procédés, I.U.T. BP 420, 44606 Saint-Nazaire Cedex, France

(*Received* 22 *January* 1990)

Abstract—Wall to liquid mass transfer coefficients are experimentally investigated, with an electrochemical method, in an annular swirling flow generated by a tangential inlet. Attention is focused on the influence of the ratio of the annular thickness e to the inlet diameter ϕ_e. According to the value of this ratio, three categories of flow regimes are obtained: the pure swirl flow, for $\phi_e = e$, the contraction swirl flow, for $\phi_e > e$ and the expansion swirl flow, for $\phi_e < e$. The other parameters of the study are the mean axial distance of the mass transfer surfaces, to characterize the swirl decay, the Reynolds number based on the hydraulic diameter and the geometric factors of the annulus. Correlations of the experimental data, taking into account the aforementioned parameters, are proposed for laminar and turbulent swirling flows.

1. INTRODUCTION

THE SWIRLING decaying flows can be achieved by different means: tangential inlets, helical inserts, tangential vanes,... [1]. The swirl is generated in the entrance section and thereafter decays freely along the flow path. The swirling flows, due to the tangential velocity component, are mainly used in exchangers, giving economy in space and more efficient heat or mass transfer than that obtained in axial pipe flow. Another application domain of the swirl flows is electrochemical engineering, and particularly for the improvement of electrochemical metal removal from dilute solutions [2]. Despite the potential applications, only a few articles are available about decaying swirling flows in an annulus.

In this work, we have determined the overall mass transfer in an annulus where the swirling decaying flow is generated by a tangential inlet tube. One of the essential parameters to characterize the generation of the swirl flow induced by tangential inlets is the initial swirl intensity which depends on the ratio between the tangential inlet diameter and the thickness of the annular gap. The original purpose of the present paper is to emphasize the influence of this ratio on hydrodynamics and mass transfer. In a previous work [3], we studied the mass transfer in different annuli where the swirl flow is generated by a tangential inlet, the diameter of which is equal to the annular thickness. The present work investigates experimentally the cases of tangential inlet diameter greater or smaller than the gap thickness; the swirl flow is associated with contraction flow or expansion flow. The presence of a step between the inlet and the annulus can induce recirculation flows [4, 5].

The objective of the investigation was to determine, using an electrochemical method, the overall mass transfer coefficients at the inner cylinder. The mass transfer section was located at different axial distances from the tangential inlet. The ratio of inlet diameter to gap thickness was varied between 0.41 and 4.96. The last parameter of the study was the Reynolds number based on the hydraulic diameter of the annulus, the investigated values of which ranged from 100 to 5900.

2. EXPERIMENTAL APPARATUS AND PROCEDURES

2.1. *Description of apparatus*

The annular cells were constituted by two concentric cylinders, 0.39 m long (see Fig. 1). The outer cylinder was made of Altuglass with a 0.025 m internal radius R_2. The inner cylinder consisted of three nickel active parts 0.1 m long, isolated from each other with inert elements. The overall mass transfer coefficients were determined at three different mean axial positions: 0.05, 0.16 and 0.27 m (see Fig. 1). Several inner cylinders with 0.018, 0.0105 and 0.008 m external radius R_1 were used to study the influence of the gap thickness $e = R_2 - R_1$ and the radius ratio $N = R_1/R_2$ (see Table 1) on the wall to liquid mass transfer. The swirl motion of the electrolyte was induced by means of different tangential inlets (see Table 1) which allowed three types of flow structures to be obtained: (i) the tangential inlet diameter ϕ_e is equal to the annular gap thickness e: the fluid movement is called 'pure swirl flow', the study of which has been detailed in ref. [3]; (ii) the inlet diameter ϕ_e is greater than the thickness e: the resulting flow is called 'contraction swirl flow'; (iii) ϕ_e is less than e: in this case we obtain the 'expansion swirl flow'.

The mean features of the test rig are given in Fig. 2. From the tank, the electrolyte, which was main-

† Author to whom correspondence should be addressed.

NOMENCLATURE

A mass transfer surface
C potassium ferricyanide concentration
D ferricyanide ion diffusion coefficient
d_H hydraulic diameter, $2e$
e annular gap thickness, $R_2 - R_1$
ERR mean square error (equation (10))
F Faraday's constant
f_e expansion factor, e/ϕ_e
$f(N), g(N)$ functions of the geometrical parameters of the annulus (equations (4) and (7))
I_l limiting diffusional current
k mass transfer coefficient
L, L_1, L_2 axial length of the mass transfer surface
L_R reattachment axial distance
$L/2e$ reduced axial coordinate
N radii ratio of the annular gap, R_1/R_2
n number of electrons involved in the electrochemical reaction
Q_v volume flow rate
R_1 external radius of the inner cylinder
R_2 internal radius of the outer cylinder
Re Reynolds number, $2e\bar{u}/\nu$
S swirl intensity (equation (15))
S_0 initial swirl intensity (equation (16))
Sc Schmidt number, ν/D
Sh Sherwood number, $2ek/D$
Sh_a, Sh_c, Sh_e, Sh_p Sherwood numbers obtained in fully developed axial flow, in contraction swirl flow, in expansion swirl flow and in pure swirl flow
T_0 swirl parameter, $\bar{v}_{id}/\bar{u}$
u, w axial, tangential velocity
$\bar{u}$ mean axial velocity in the annulus
$\bar{v}_{id}$ mean axial velocity in the inlet duct
x axial distance from the inlet.

Greek symbols
ν kinematic viscosity of the electrolyte
ρ density of the electrolyte
ϕ_e diameter of the tangential inlet.

tained at the constant temperature of 30°C, flowed through a centrifugal pump to the two flowmeters which allowed the measurement of the volume flow rate in a range of 0.020–1 $m^3 h^{-1}$. Then, the electrolyte entered the vertical test cell tangentially and was recycled to the tank by means of a tangential outlet.

2.2. *Electrochemical method*

The overall mass transfer was performed using a polarographic method. The electrolyte was an aqueous solution of 2×10^{-3} M potassium ferricyanide, 5×10^{-2} M potassium ferrocyanide and 0.5 M sodium hydroxide. At 30°C, the physical properties of the electrolyte are: density $\rho = 1028$ kg m^{-3}, kinematic viscosity $\nu = 8.73 \times 10^{-7}$ m^2 s^{-1} and diffusion coefficient of ferricyanide ions in the electrolyte $D = 6.95 \times 10^{-10}$ $m^2 s^{-1}$. The studied electrochemical reaction was the reduction of the ferricyanide ions. The mass transfer coefficient k was determined under diffusion controlled conditions on the cathode, thus k was related to the limiting current I_L by

$$k = I_l/(nFAC). \quad (1)$$

One of the three nickel parts of the inner cylinder acted alternately as the cathode, the other two acted as the anode. The reference electrode consisted of a platinum wire.

The interest of this experimental method is that the mass transfer surface remains unchanged during the experiments. Moreover, the boundary condition of the mass transfer experiments, uniform concentration

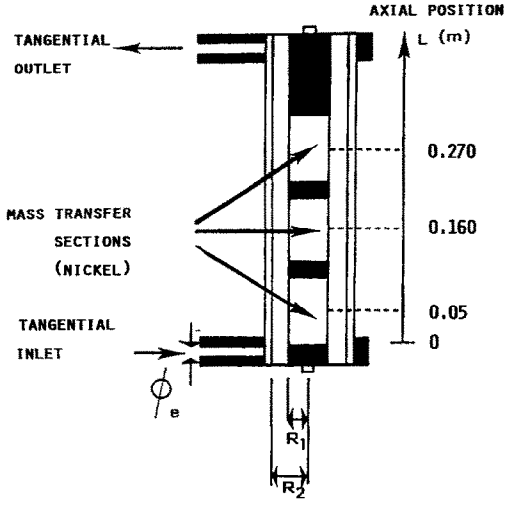

FIG. 1. General view of the test annular cell.

Table 1. Geometric characteristics of the annuli and tangential inlets

Inner cylinder radius, R_1 (m)	Gap thickness, $e = R_2 - R_1$ (m)	Radius ratio, $N = R_1/R_2$	Tangential inlet diameter, ϕ_e (m)
0.0180	0.0070	0.72	0.0070 0.0090 0.0125 0.0347
0.0105	0.0145	0.42	0.0070 0.0145
0.0080	0.0170	0.32	0.0070 0.0170

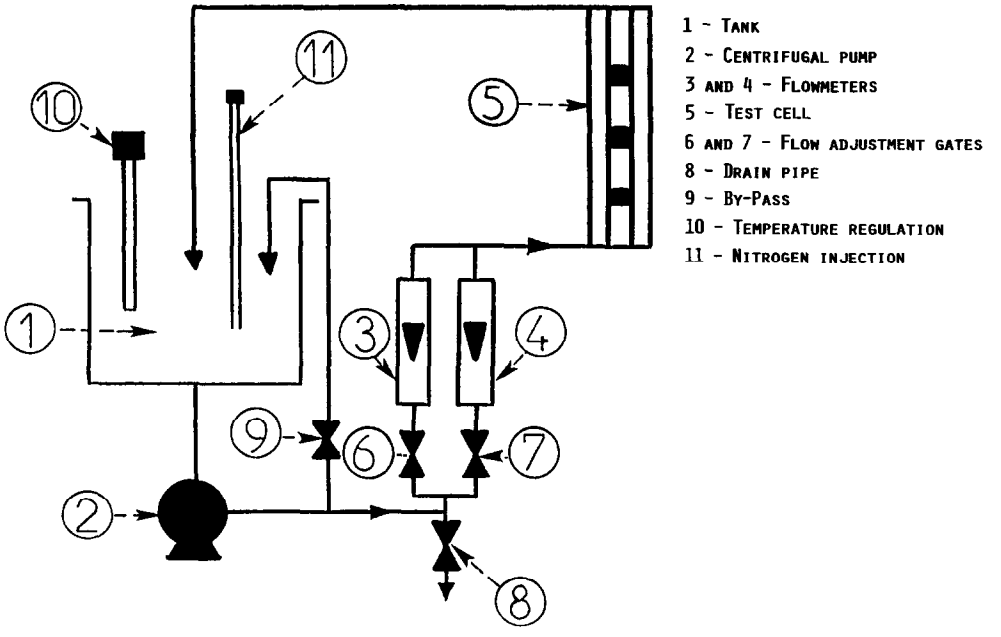

FIG. 2. Schematic layout of the experimental facility.

at the electrodes ($C = 0$ for the diffusion controlled conditions), corresponds to uniform temperature at the same heat transfer surface. Thereby, the mass transfer results could be applied to heat transfer problems for analogous hydrodynamic conditions.

3. MASS TRANSFER IN THE PURE SWIRL FLOW

The pure swirl flow is obtained when the tangential inlet diameter is equal to the annulus gap thickness (Fig. 3). Three configurations have been used in the study: $\phi_e = R_2 - R_1 = 0.007, 0.0145$ and 0.017 m. The results obtained in this type of flow were reported in ref. [3]. From a mass transfer point of view, two flow regimes have been observed (Fig. 4). For $Re < 1000$, the Sherwood number varied with $Re^{0.5}$; this variation was found to be similar to that obtained in the developing laminar axial flow [6]. The experimental data obtained in the three different geometries have been correlated, for $Re < 1000$, by the following equation:

$$Sh_p = 2.50 Re^{0.5} Sc^{1/3} \left[\frac{L}{2e}\right]^{-0.23} \left[\frac{\bar{v}_{id}}{\bar{u}}\right]^{0.3} \quad (2)$$

where $L/2e$ ($1.5 \leqslant L/2e \leqslant 19.3$) is the mean non-dimensional length from the inlet and $\bar{v}_{id}/\bar{u}$ the ratio of the mean tangential inlet velocity to the mean annular axial velocity.

For $Re > 2000$, all the experimental points have been correlated by

$$Sh_p = 0.14 Re^{0.8} Sc^{1/3} \left[\frac{L}{2e}\right]^{-0.26} [f(N)]^{0.16}. \quad (3)$$

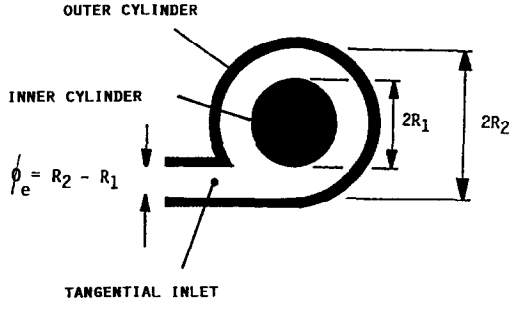

FIG. 3. Sketch of the tangential inlet—case of the pure swirl flow.

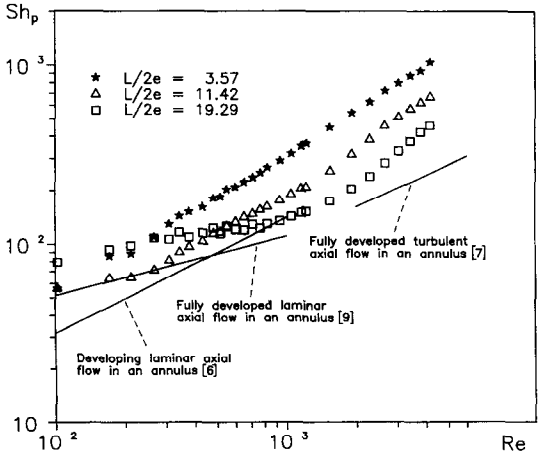

FIG. 4. Mass transfer results of pure swirl flow for $N = 0.72$ and $\phi_e = 0.007$ m.

The Sherwood number was proportional to $Re^{0.8}$ as for the developed turbulent flow in a pipe. The parameter $f(N)$ is the same geometrical function as the one used by Ross and Wragg [7] to express the annular turbulent mass transfer, so

$$f(N) = \left[\frac{1-N}{1-\delta^2}\right]^{0.2}\left[\frac{\delta^2-N^2}{N(1-\delta^2)}\right] \quad (4)$$

with

$$\delta^2 = \frac{1-N^2}{2\ln(1/N)}. \quad (5)$$

4. MASS TRANSFER IN THE CONTRACTION SWIRL FLOW

The influence of the tangential inlet diameter ϕ_e was studied in the annular cell defined by the gap thickness $e = 0.007$ m. Three tangential inlet diameters were used: $\phi_e = 0.009$, 0.0125 and 0.0347 m. The value of ϕ_e was always greater than e, thus the tangential inlet and the annulus formed a fluid contraction (see Fig. 5). During the experiments the Reynolds number was varied between 100 and 5500.

4.1. *Influence of the axial position of the mass transfer section*

The Sherwood number is plotted in Fig. 6 for the three positions of the transfer section and for the tangential inlet diameter $\phi_e = 0.0125$ m. At a given Reynolds number, the average mass transfer decreases with the axial distance of the mass transfer section. This result is particularly significant for large Reynolds numbers. In this case ($Re > 2000$), the tangential component of the velocity is important and its influence on the mass transfer coefficients is sensitive up to the upper transfer surface. The decrease of mass transfer with the axial distance is a result of swirl decay along the flow path [3, 8].

As for pure swirl flow [3], two flow regimes, one for $Re < 1000$ and the second for $Re > 2000$, are clearly shown on Fig. 6. The increase of the mass transfer coefficients due to the contraction swirl flow by comparison with the developed axial flow is shown on Fig. 7, where the axial distribution of the ratio Sh_c/Sh_a is given. The axial Sherwood number Sh_a is calculated for $Re < 1000$ with the Turitto equation [9]

$$Sh_a = 1.0[2g(N)\,Re\,Sc\,e]^{1/3}\left[\frac{L_2^{2/3}-L_1^{2/3}}{L_2-L_1}\right] \quad (6)$$

where

$$g(N) = \frac{2\left[-2N^2+\dfrac{1-N^2}{\ln(1/N)}\right]\left[\dfrac{1-N}{N}\right]}{1+N^2-\left[\dfrac{1-N^2}{\ln(1/N)}\right]}. \quad (7)$$

For $Re > 2000$, Sh_a is given by Ross and Wragg [7] who have determined the turbulent annular mass transfer by assuming a linear velocity distribution in the boundary layer, hence

$$Sh_a = 0.807Sc^{1/3}\,Re^{0.6}[0.046f(N)]^{1/3} \times (2e)^{1/3}\left[\frac{L_2^{2/3}-L_1^{2/3}}{L_2-L_1}\right] \quad (8)$$

where $f(N)$ is defined by equation (4).

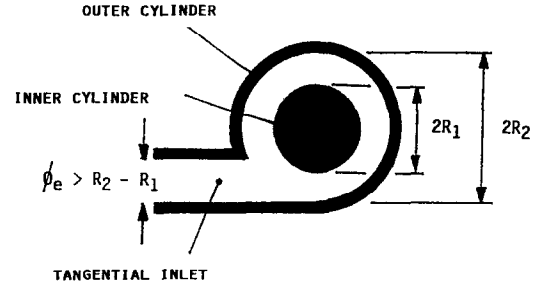

FIG. 5. Sketch of the tangential inlet—case of the contraction swirl flow.

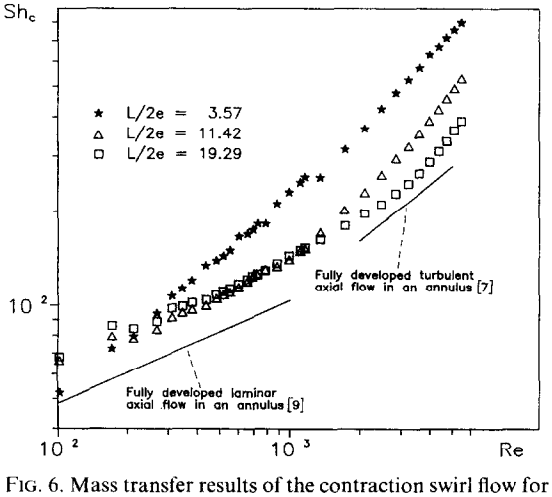

FIG. 6. Mass transfer results of the contraction swirl flow for $N = 0.72$ and $\phi_e = 0.0125$ m.

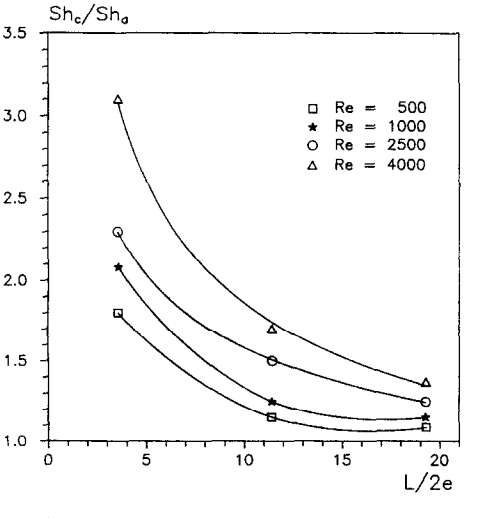

FIG. 7. Axial distribution of Sh_c/Sh_a for $N = 0.72$ and $\phi_e = 0.125$ m.

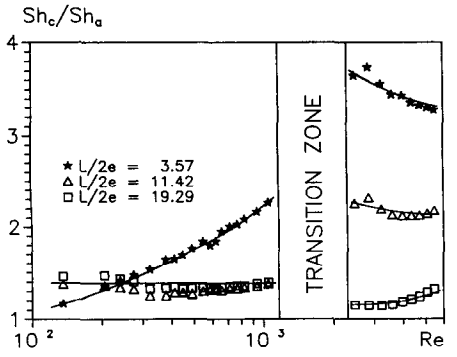

FIG. 8. Effect of Reynolds number on Sh_c/Sh_a for $N = 0.72$ and $\phi_e = 0.0125$ m.

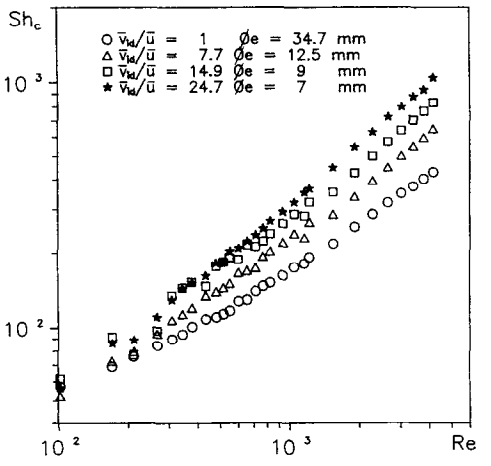

FIG. 9. Effect of the tangential inlet diameter on the mass transfer for $N = 0.72$ and $0 < L < 0.1$ m.

For the lowest position of the mass transfer surface ($L/2e = 3.57$), the relative increase of mass transfer coefficients is important: for $Re = 4000$, $Sh_c/Sh_a > 3$ (Fig. 6). The influence of the swirl motion is sensitive even for low Reynolds numbers. On the contrary, when the value of $L/2e$ increases, the values of the mass transfer coefficient tend to those obtained in pure axial flow: $Sh_c/Sh_a \simeq 1$ for $L/2e = 19.29$ and for all Reynolds numbers. For the upper position of the transfer section and particularly for $100 < Re < 1000$, we can consider that the swirl is completely decayed, but the axial velocity profile is no well established. In this last case, the mass transfer is more important than the one obtained in the fully developed laminar axial flow [10].

The effect of Reynolds number on the ratio Sh_c/Sh_a is shown in Fig. 8, for the inlet diameter $\phi_e = 0.0125$ m. For $Re > 2000$, Sh_c/Sh_a is nearly independent of Re, therefore the evolution of the mass transfer with Re is similar in the contraction swirl flow and the turbulent axial flow. The same conclusion can be drawn for $Re < 1000$, except for the lowest transfer surface, for which Sh_c/Sh_a increases with Re, hence the swirl Sherwood number Sh_c varies with Re^a, with $a > 1/3$.

4.2. *Influence of the tangential inlet diameter*

The increase of the inlet diameter improves the mass transfer (Fig. 9). This behaviour corresponds to the decrease of the initial swirl intensity, which is described [3] by a swirl parameter T_0 defined by the ratio of the tangential inlet velocity $\bar{v}_{id}$ to the mean annular velocity $\bar{u}$. In particular, the mass transfer coefficients obtained in the pure swirl flow are higher than those obtained in the contraction swirl flow ($\phi_e = 0.007$ m). For small Reynolds numbers ($Re < 500$), the Sherwood number slightly decreases when the inlet diameter increases. In contrast, for $Re > 1000$, the Sherwood number has a strong dependence on the swirl parameter: when $\bar{v}_{id}/\bar{u}$ varies from 1 to 24.7, the Sherwood numbers are multiplied by a factor of 2.5.

For $Re < 1000$, the ratio of contraction swirl Sherwood numbers Sh_c to the one obtained in the pure swirl flow Sh_p decreases rapidly when the Reynolds number increases (Fig. 10). Thus the swirl decay is very sensitive to the inlet type. But for high values of Re ($Re > 2000$), the ratio Sh_c/Sh_p is nearly constant, the swirl is slightly decayed, even for the contraction swirl flow.

4.3. *Correlation of the experimental data*

All the experimental data have been correlated using the same type of equation—one for $Re < 1000$ and one for $Re > 2000$—as those defined for the pure swirl flow (equations (2) and (3)). The equations of correlation take into account the different parameters influencing the mass transfer:

(a) $L/2e$, to characterize the swirl decay,
(b) $T_0 = \bar{v}_{id}/\bar{u}$, for the swirl parameter,
(c) the Reynolds number.

The different parameters of the correlation are determined simultaneously by means of multi-linear

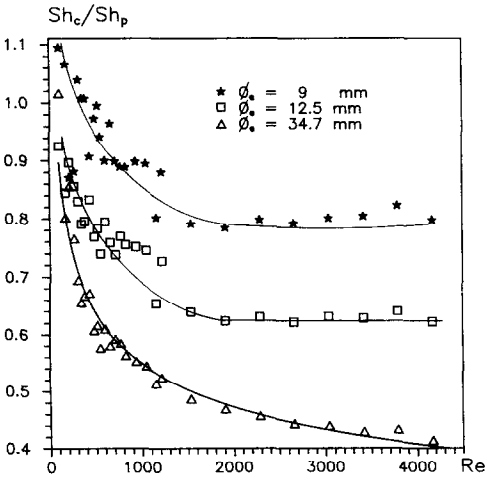

FIG. 10. Influence of the tangential inlet diameter. Re related to Sh_c/Sh_p for $N = 0.72$ and $0 < L < 0.1$ m.

regression. The accuracy of our correlations is evaluated with the relative mean square error ERR

$$ERR = \left[\frac{1}{N_{exp}}\sum_{i=1}^{N_{exp}}\frac{[Sh_i^{calc} - Sh_i^{exp}]^2}{[Sh_i^{exp}]^2}\right]^{1/2} \quad (9)$$

where N_{exp} is the number of experimental data, Sh_i^{calc} the value of Sh calculated using the correlation and Sh_i^{exp} the value of the experimental Sherwood number.

For $Re < 1000$, we obtained

$$Sh_c = 0.99 Re^{0.43} Sc^{1/3}\left[\frac{L}{2e}\right]^{-0.11} T_0^{0.017} \quad (10)$$

with an error $ERR = 15\%$ for 311 experimental data. Equation (10) was determined in the following experimental domain: $100 \leqslant Re \leqslant 1000$, $3.6 \leqslant L/2e \leqslant 19.3$, $1 \leqslant T_0 \leqslant 24.6$, $N = 0.72$. The comparison of equations (2) and (10) shows that the swirl decay and thus the mass transfer decrease is faster in the pure swirl flow ($Sh_p \propto [L/2e]^{-0.23}$, equation (2)) than in the contraction swirl flow ($Sh_c \propto [L/2e]^{-0.11}$, equation (10)). This result is due to the fact that the initial swirl intensity is more important in the pure swirl flow. Further inspection of equation (10) shows that the mass transfer is quasi-independent of the swirl parameter ($Sh \propto T_0^{0.017}$). Sh_c increases with T_0 ($Sh_c \propto T_0^{0.017}$), contrary to the case of the pure swirl flow ($Sh_p \propto T_0^{-0.28}$, equation (2)). It seems that the parameter T_0 is not sufficient to characterize the initial swirl intensity.

For $Re > 2000$, the experimental data have been correlated by

$$Sh_c = 0.091 Re^{0.80} Sc^{1/3}\left[\frac{L}{2e}\right]^{-0.39} T_0^{0.18} \quad (11)$$

with $ERR = 9.2\%$ and $N_{exp} = 156$. Equation (11) can be applied for: $2000 \leqslant Re \leqslant 5900$, $3.6 \leqslant L/2e \leqslant 19.3$, $1 \leqslant T_0 \leqslant 24.6$, $N = 0.72$. This correlation shows that the mass transfer strongly depends on the axial position of the mass transfer surface.

The only available data dealing with the contraction swirl flow have been obtained by Shoukry and Shemilt [8] in an annulus of 0.0127 m gap thickness and a 0.01905 tangential inlet diameter. The experimental points of ref. [8] are reported on Fig. 11, and we can see that those data are well predicted by equation (11).

Equation (11) is also compared with the correlation of Garcia and Sparrow [4], obtained for turbulent mass transfer downstream of a contraction-related, forward-facing step in a duct. In the presence of a contraction, the axial distribution of the Sherwood number increased at first, reached a maximum value and then decreased to the fully developed value. The maximum value of the Sherwood number is located at about $x/2e = 0.5$; x is the axial distance from the abrupt contraction. The effect of the contraction ratio on peak Sherwood number is very small [4] and the peak values can be correlated by

$$Sh = 0.26 Re^{0.69} Sc^{1/3}. \quad (12)$$

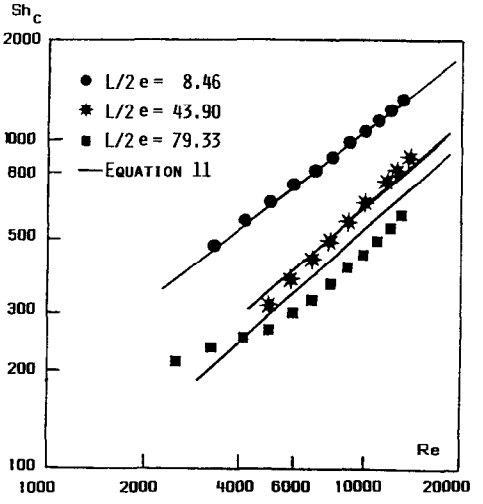

FIG. 11. Mass transfer in contraction swirl flow. Comparison with the experimental data of ref. [8].

Applying our correlation (equation (11)) to this problem with $T_0 = 1$ and $L/2e = 0.5$, we obtain

$$Sh = 0.12 Re^{0.80} Sc^{1/3}. \quad (13)$$

The mass transfer in contraction swirl flow is meaningfully higher for $Re > 2000$ than in contraction axial flow. This result proves the interest of the swirl flow. Due to the fact that the axial position of the peak is very close to the contraction, the presence of the peak is not detected in the experimental determination of the overall mass transfer.

5. GENERAL CORRELATION FOR THE OVERALL MASS TRANSFER IN PURE AND CONTRACTION SWIRL FLOWS

5.1. *Choice of the equation of correlation*

To the best of the author's knowledge, no general correlation for mass/heat transfer in swirling decaying flows induced by tangential inlets is available. The correlations of the literature are very often given in terms of: Sh (or Nu) $= a\,Re^b$, where a and b depend on all the other factors influencing the mass (or heat) transfer [11]. It is difficult to establish a generally applicable selection of these factors but the correlation has to take into consideration the fact that the swirl Sherwood number Sh_p (or Sh_c) tends to the axial Sherwood number Sh_a when the axial distance $L/2e$ increases. Thus, the chosen correlation has the same form as the one used by Hay and West [12] for the heat transfer in swirling pipe flow induced by a rectangular tangential inlet, therefore

$$\frac{Sh}{Sh_a} = (1+S)^a \quad (14)$$

where S is the swirl intensity defined by

$$S = \frac{\int_{R_1}^{R_2} \rho r^2 uw \, dr}{R_2 \int_{R_1}^{R_2} \rho r u^2 \, dr}. \quad (15)$$

S represents the ratio of the local flux of angular momentum to the flux of axial momentum. In order to determine S, it is necessary to know the axial and tangential velocity profiles for all the axial positions. The problem is solved by modelling the swirl intensity S by

$$S = S_0 \left[\frac{L}{2e}\right]^c. \quad (16)$$

The term $[L/2e]^c$, with $c < 0$, characterizes the swirl decay, as shown by equations (2) and (3) for the pure swirl flow and by equations (10) and (11) for the contraction swirl flow. The term S_0 represents the initial swirl intensity; the definition of S_0 is different from T_0, because this last parameter does not describe adequately the swirl intensity (see Section 4.3). We have established that the initial swirl intensity is related to the mean velocity $\bar{v}_{id}$ in the tangential inlet, therefore we have expressed S_0 by a Reynolds number based on $\bar{v}_{id}$

$$S_0 \sim \frac{2e\bar{v}_{id}}{\nu}. \quad (17)$$

The mean tangential inlet velocity $\bar{v}_{id}$ is given by

$$\bar{v}_{id} = \frac{4Q_v}{\Pi \phi_e^2}. \quad (18)$$

Combining equations (17) and (18) yields

$$S_0 \sim \frac{4(1+N)}{1-N}\left[\frac{e}{\phi_e}\right]^2 Re. \quad (19)$$

Thus, the equation of correlation (14) becomes

$$\frac{Sh}{Sh_a} = \left[1 + d\left[\frac{4(1+N)}{1-N}\left(\frac{e}{\phi_e}\right)^2 Re\right]^b \left(\frac{L}{2e}\right)^c\right]^a. \quad (20)$$

Parameters a, b, c and d are determined by using the Rosenbroock algorithm [13] in order to minimize the error between the calculated Sherwood numbers (equation (20)) and the experimental Sherwood numbers.

5.2. *Results*

All the experimental data, obtained in the pure and contraction swirl flows are correlated together. Two equations of the correlation are proposed, one for $Re < 1000$ and the other for $Re > 2000$. For both equations, the parameter a of equation (20) is found to be nearly equal to 1 : $a = 0.98$ for $Re < 1000$ and $a = 1.04$ for $Re > 2000$. Thereby, the value of a is taken equal to 1 in both equations.

For $Re < 1000$, the equation

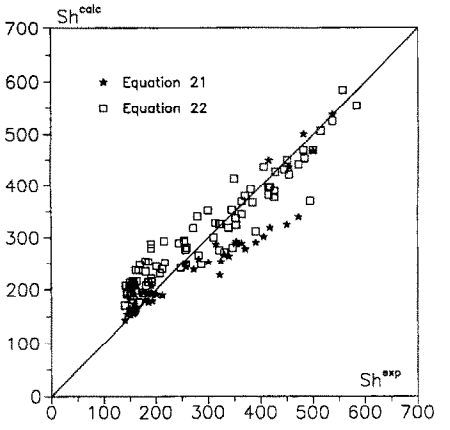

FIG. 12. Comparison of prediction equations with experimental results obtained in pure and contraction swirl flows for $1000 < Re < 2000$.

$$\frac{Sh}{Sh_a} = 1 + 0.5\left[\frac{4(1+N)}{1-N}\left(\frac{e}{\phi_e}\right)^2 Re\right]^{0.18}\left(\frac{L}{2e}\right)^{-0.7} \quad (21)$$

correlates the 611 experimental points with a good fitness ($ERR = 16\%$). The experimental domain corresponding to the correlation is: $100 \leqslant Re \leqslant 1000$, $1.47 \leqslant L/2e \leqslant 19.3$, $0.04 \leqslant (e/\phi_e)^2 \leqslant 1$, $0.32 \leqslant N \leqslant 0.72$.

For $Re > 2000$, the proposed correlation is

$$\frac{Sh}{Sh_a} = 1 + 0.32\left[\frac{4(1+N)}{1-N}\left(\frac{e}{\phi_e}\right)^2 Re\right]^{0.18}\left(\frac{L}{2e}\right)^{-0.31}. \quad (22)$$

The correlation is obtained for 294 experimental points. The fit between predicted and experimental values of the Sherwood number is quite good and it is obtained with a mean square error $ERR = 21\%$. The experimental domain is: $2000 \leqslant Re \leqslant 5900$, $1.47 \leqslant L/2e \leqslant 19.3$, $0.04 \leqslant (e/\phi_e)^2 \leqslant 1$, $0.32 \leqslant N \leqslant 0.72$.

A comparison of equations (21) and (22) shows that the effect of the initial swirl intensity S_0 is the same in both flow regimes, but the swirl intensity decreases more rapidly in the laminar regime.

For $1000 < Re < 2000$, we have plotted in Fig. 12 the variations of the Sherwood numbers calculated using equations (21) and (22) with the measured Sherwood numbers (220 experimental points). The experimental values of Sh are well predicted by both equations. Thus the domain defined by $1000 < Re < 2000$ corresponds to an intermediate flow regime.

6. MASS TRANSFER IN THE EXPANSION SWIRL FLOW

The hydrodynamic conditions studied below deal with the setup of an abrupt asymmetric enlargement between the tangential inlet and the annulus (Fig. 13). The annulus consists of an outer cylinder of radius equal to 0.025 m and two different nickel inner cylinders with radii of 0.0105 and 0.008 m. The tangential inlet diameter is equal to 0.007 m for the two annuli,

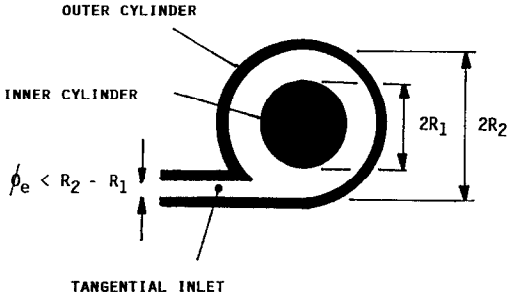

FIG. 13. Sketch of the tangential inlet—case of the expansion swirl flow.

therefore $e = R_2 - R_1$ is always higher than ϕ_e and we can consider that the fluid flow conditions result from the association of the tangential inlet with the sudden asymmetric expansion. With regard to literature, there do not seem to be prior mass/heat transfer results for this hydrodynamic situation. The mass transfer coefficients were obtained for a variation of the Reynolds numbers between 120 and 4600.

6.1. *Axial distribution of the mass transfer*

Three mean axial positions of the mass transfer section have been investigated: $L = 0.05$, 0.16 and 0.27 m. The variation of Sherwood–Reynolds numbers is plotted on Fig. 14 for $N = 0.42$ and for the three non-dimensional axial positions. Contrary to the cases of pure and contraction swirl flows, the mass transfer does not decrease monotonically with the increase of $L/2e$. For example, the Sherwood number measured at the lowest mass transfer surface ($0 \leqslant L \leqslant 0.1$ m) is less than the one obtained for the intermediate position of the test section ($0.11 \leqslant L \leqslant 0.21$ m), otherwise the last one is higher than the Sherwood number determined at the upper transfer station. The mass transfer rises in the region immediately downstream of the expansion, achieves a maximum, and thereafter decreases toward the fully developed axial mass transfer.

This behaviour is similar to that obtained downstream of hydrodynamic singularities such as axisymmetric sudden expansions [5], where recirculation flows in laminar and turbulent regimes exist. The mass transfer evolutions correspond to the separation, reattachment, redevelopment sequence experienced by the flow. The recirculation flow persists up to the reattachment of the separated flow to the wall. The fluid recirculation in swirl flows has been also studied by Hallet and co-workers [14, 15], who visualized the flow downstream of an axisymmetric sudden expansion. The swirl flow is generated in a tube with four tangential inlets associated with an axial one. They established that the appearance of the recirculation zone was related to the initial swirl intensity S_0. The critical value of S_0 for the presence of the separated flow is decreased with increasing expansion factor f_e. Dellenback *et al.* [16] investigated the local heat transfer rates in tube swirl flow downstream of an axisymmetric abrupt expansion. In the turbulent recirculation region, the local heat transfer magnitude is 3–9.5 times larger than fully developed axial flow values. The magnitude of the peak mass/heat transfer is dependent of both Re and f_e [5, 14]. In our experimental conditions, the enhancement of the overall mass transfer is noteworthy, the normalized Sherwood number Sh_e/Sh_a varies between 1.5 and 4.0 (Fig. 15).

6.2. *Influence of the geometric factors*

The Sherwood number measured at the highest mass transfer section is less than that obtained at the lowest mass transfer surface ($N = 0.42$, Fig. 14). The opposite result is shown on Fig. 16 for $N = 0.32$. When the radius ratio decreases, and thus the expansion factor $f_e = e/\phi_e$ increases, the axial location of the peak Sherwood number is increased. Analogous

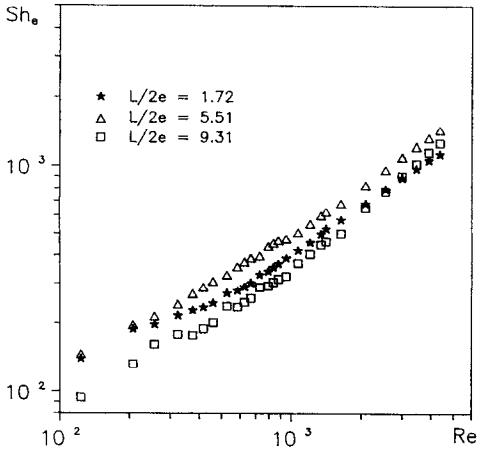

FIG. 14. Mass transfer results of the expansion swirl flow for $N = 0.42$ and $f_e = 2.07$.

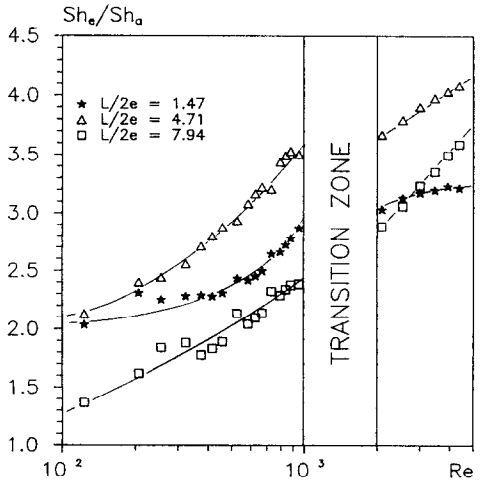

FIG. 15. Variation of the normalized Sherwood number Sh_e/Sh_a with Re for $N = 0.42$ and $f_e = 2.07$.

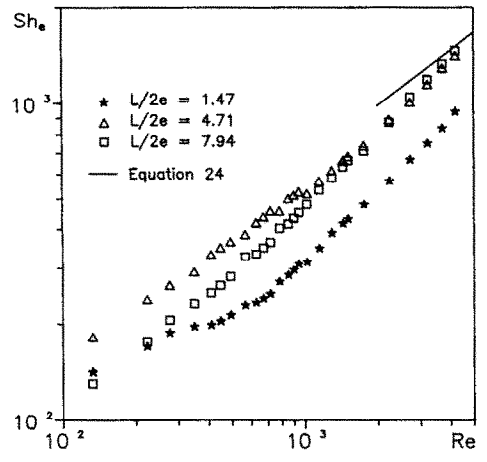

FIG. 16. Mass transfer results of the expansion swirl flow for $N = 0.32$ and $f_e = 2.43$.

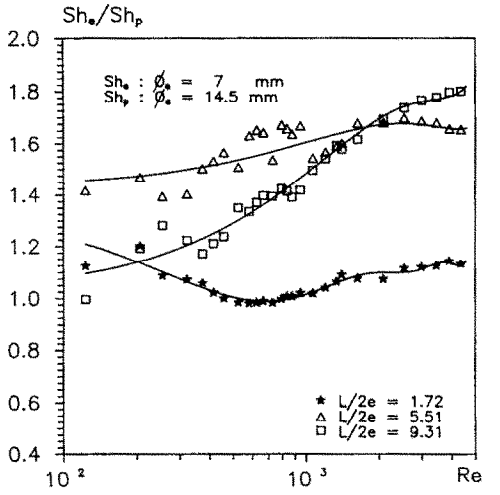

FIG. 17. Variation of Sh_e/Sh_p with Re for $N = 0.72$.

results were obtained in previous studies. The location of maximum mass/heat transfer occurs upstream of the flow reattachment point [15, 16], it moves slightly downstream with increasing expansion factor f_e [5, 17]. The influence of the Reynolds number is not clearly established. Dellenback *et al.* [16] found in the expansion swirl flow that the location of the maximum showed little dependence on the Reynolds number. Otherwise, Sparrow and Chuck [18], for flow downstream of an abrupt and asymmetric enlargement in a channel, correlated the reattachment distance L_R by

$$\frac{L_R}{h} = (0.249 - 0.0626 f_e)\frac{f_e - 1}{f_e}[Re_h(f_e - 1)]^{0.777} \quad (23)$$

where h is the height of the enlarged channel and $Re_h = \bar{u}h/\nu$, with $Re_h < 900$. According to this equation, L_R/h exhibits a strong dependence on Re_h. Wragg *et al.* [5], for nozzle flows expanding into an axisymmetric circular or square duct, observed a similar behaviour. The reason for the two distinct effects of Reynolds number could be explained by the presence of swirl flows in ref. [15]. It will be worthwhile to explore this problem.

Wragg *et al.* [5] determined experimentally the maximum local mass transfer for $Re > 3000$. Peak mass transfer data for both square and circular geometries can be correlated by the following expression:

$$Sh_{e\max} = 0.55 Sc^{1/3}(Re\, f_e)^{0.60}. \quad (24)$$

This correlation equation is reported in Fig. 16 with our experimental data, and we can see that the agreement is good. It means that the expansion swirl flow mass transfer is significantly higher than expansion axial flow mass transfer, because equation (24) predicts the maximum Sherwood number, whereas the experimental data represents mean measures on mass transfer surface 0.1 m long. It is also noteworthy that the peak Sherwood number is significantly higher in axial expansion flow (equation (24)) than in contraction flow (equation (12)).

Figure 17 shows the evolution of the ratio of the expansion swirl Sherwood number Sh_e to the pure swirl Sherwood number Sh_p for $N = 0.42$. For the two lowest mass transfer stations, the ratio Sh_e/Sh_p is quasi-independent of the Reynolds number. Otherwise, for the highest transfer surface, Sh_e/Sh_p increases with Re. The same results have been obtained for $N = 0.32$ [11]. In the recirculation zone, the flow regime is not very sensitive to the Reynolds number, thus Sh_e/Sh_p is nearly constant with increasing Re. After the reattachment point, there is the redevelopment of the swirl flow; the recirculation zone involves a delay to the swirl flow. Thus, for a given axial distance located downstream of the reattachment point, the ratio Sh_e/Sh_p increases with Re because the decay of the expansion swirl flow begins at a distance $x = L_R$, namely after the decay of the pure swirl flow which begins as soon as the fluid enters the annulus. It is interesting to note that, for the three different mass transfer surface positions, the mass transfer in expansion swirl flow is greater than in pure swirl flow.

6.3. *Correlation of the experimental data*

It is established that the swirl flow is redeveloped after the reattachment point of the separated flow, so that the empirical correlations determined in the pure and contraction swirl flows (equations (21) and (22)) can be used for the expansion swirl flow downstream of the recirculation zone, by replacing the parameter $L/2e$ by $(L - L_R)/2e$. A local study of the expansion swirl flow will be necessary to find L_R exactly. In the first approximation, we have assumed that the recirculation zone is essentially located near the lowest transfer surface for the two annuli ($N = 0.32$ and 0.42), therefore the decaying swirling flow begins at the leading edge of the intermediate transfer surface: $L_R = 0.11$ m. Applying equation (23) to our exper-

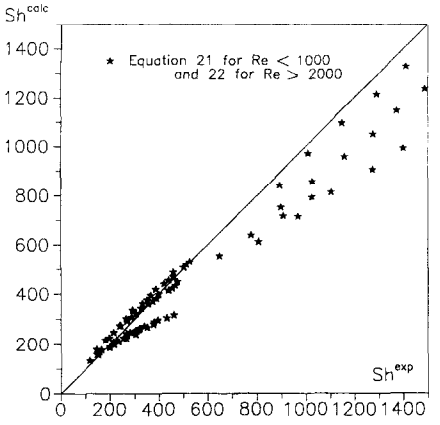

FIG. 18. Comparison between the correlation established for pure and contraction swirl flows and experimental data obtained in expansion swirl flow.

imental conditions, we obtained high values of the reattachment distance: for $Re = 300$ and $N = 0.42$, $L_R = 0.48$ m. However, according to the fact that the swirl flow is generated by a tangential inlet, the real axial reattachment distance travelled by a fluid particle is much smaller. Furthermore, Dellenback *et al.* [16] have shown that the peak mass/heat transfer moves significantly upstream as swirl strength is increased; for example the peak axial distance is divided by four when the swirl number varies between 1 and 0 (pure axial flow).

The comparison between the experimental and calculated (with equations (21) and (22)) Sherwood numbers is given in Fig. 18. For low Sherwood numbers, or for $Re < 1000$, the experimental data are well correlated by equation (21). Then, for $Re > 2000$, equation (22) predicts mass transfer coefficients lower than the experimental values, namely L_R is underestimated by the foregoing value. This result is probably due to the discrepancy on the value of L_R, which depends on the Reynolds number and on the expansion factor e/ϕ_e. The good agreement between the empirical correlations and the experimental data proves that the swirl flow is actually redeveloped after the recirculation zone.

7. CONCLUSION

According to the ratio of tangential inlet diameter ϕ_e to the annular thickness e, overall wall to liquid mass transfer performed in annular geometries provided the definition of three different flow regimes:

(1) the pure swirl flow when $\phi_e = e$,
(2) the contraction swirl flow for $e/\phi_e < 1$,
(3) the expansion swirl flow for $e/\phi_e > 1$.

The first two flows are similar from a mass transfer point of view, they can be considered as swirling decaying flows. The mass transfer coefficients in the pure swirl flow are higher than those attainable in contraction swirl flow, due to the initial swirl intensity, which decreases with decreasing e/ϕ_e.

In the expansion swirl flow, there is a recirculation zone just downstream of the entrance, and then the swirl flow is redeveloped. The mass transfer is more important than the one in the two other types of swirl flow. This result confirms that the ratio e/ϕ_e is the right parameter to characterize the initial swirl intensity. Moreover, e/ϕ_e also represents the expansion factor, which is the main parameter to describe the sudden expansion fluid flow.

For the pure and contraction swirl flows, two general correlations are proposed, for laminar and turbulent regimes, taking into account the initial swirl intensity and the fact that the swirl flow decays towards the developed axial flow. All the experimental data are expressed with a satisfactory accuracy by the correlations. The data obtained downstream of the recirculation zone in the expansion swirl flow are also well correlated by the proposed empirical correlations. The expansion swirl flow can be described by a recirculation zone, which is related to the sudden expansion axial flows features, followed by a pure swirling decaying flow. Further local investigations should provide information about the expansion swirl flows which could be very useful in heat/mass exchangers, due to the significant increase of heat/mass transfer rates over those found in purely axial flow, and even in pure swirl flows.

REFERENCES

1. A. K. Gupta, D. G. Lilley and N. Syred, *Swirl Flows*. Abacus, Cambridge (1984).
2. F. C. Walsh and G. Wilson, The electrolytic removal of gold from spent electroplating liquors, *Trans. IMF* **64**, 55–61 (1986).
3. P. Legentilhomme and J. Legrand, Overall mass transfer in swirling decaying flow in annular electrochemical cells, *J. Appl. Electrochem.* **20**, 216–222 (1990).
4. A. Garcia and E. M. Sparrow, Turbulent heat transfer downstream of a contraction-related, forward-facing step in a duct, *J. Heat Transfer* **109**, 621–626 (1987).
5. A. A. Wragg, D. J. Tagg and M. A. Patrick, Diffusion-controlled current distributions near cell entries and corners, *J. Appl. Electrochem.* **10**, 43–47 (1980).
6. F. Coeuret et A. Storck, *Eléments de Génie Electrochimique*. Lavoisier, Paris (1984).
7. T. K. Ross and A. A. Wragg, Electrochemical mass transfer studies in annuli, *Electrochim. Acta* **10**, 1093–1106 (1965).
8. E. Shoukry and L. W. Shemilt, Mass transfer enhancement in swirling annular pipe flow, *Ind. Engng Chem. Process. Des. Dev.* **24**, 53–56 (1985).
9. V. T. Turitto, Mass transfer in annuli under conditions of laminar flow, *Chem. Engng Sci.* **30**, 503–509 (1974).
10. M. Ould-Rouis, C. Nouar, A. Salem, J. Legrand and P. Legentilhomme, Hydrodynamics and mass transfer of the laminar flow in the entrance region of an annular electrochemical reactor, *Ind. Chem. Engng Symp. Ser.* **12**, 17–28 (1989).
11. P. Legentilhomme, Hydrodynamique et transfert de matière de l'écoulement annulaire tourbillonnaire produit par une entrée tangentielle du fluide, Thesis, University of Nantes (1991).

12. N. Hay and P. D. West, Heat transfer in free swirling flow in a pipe, *J. Heat Transfer* 411–416 (1975).
13. G. S. G. Beveridge and R. S. Schechter, *Optimization: Theory and Practice*. McGraw-Hill, New York (1970).
14. W. L. H. Hallet and R. Günter, Flow and mixing in swirling flow in a sudden expansion, *Can. J. Chem. Engng* **62,** 149–155 (1984).
15. W. L. H. Hallet and D. J. Toews, The effects of inlet conditions and expansion ratio on the onset of flow reversal in swirling flow in a sudden expansion, *Exp. Fluids* **5,** 129–133 (1987).
16. P. A. Dellenback, D. E. Metzger and G. P. Neitzel, Heat transfer to turbulent swirling flow through a sudden axisymmetric expansion, *J. Heat Transfer* **109,** 613–620 (1987).
17. E. M. Sparrow, S. S. Kong and W. Chuck, Relation between the points of flow reattachment and maximum heat transfer for regions of flow separation, *Int. J. Heat Mass Transfer* **30,** 1237–1246 (1987).
18. E. M. Sparrow and W. Chuck, PC solutions for heat transfer and fluid flow downstream of an abrupt asymmetric enlargement in a channel, *Numer. Heat Transfer* **12,** 19–40 (1987).

INFLUENCE DES CONDITIONS D'ENTREE SUR LE TRANSFERT DE MATIERE DANS LES ECOULEMENTS ANNULAIRES TOURBILLONNAIRES NON ENTRETENUS

Résumé—Les coefficients de transfert de matière liquide-paroi ont été déterminés expérimentalement à l'aide d'une méthode électrochimique dans un écoulement annulaire tourbillonnaire induit par une entrée tangentielle. L'étude porte plus particulièrement sur l'influence du rapport de l'épaisseur de l'espace annulaire e au diamètre de l'entrée ϕ_e. Selon la valeur de ce rapport, trois types d'hydrodynamique sont mis en évidence: l'écoulement tourbillonnaire pur, pour $\phi_e = e$, l'écoulement tourbillonnaire avec contraction, pour $\phi_e > e$ et l'écoulement tourbillonnaire avec expansion, pour $\phi_e < e$. Les autres paramètres de l'étude sont la distance axiale moyenne des surfaces de transfert par rapport à l'entrée, pour caractériser la décroissance de l'intensité tourbillonnaire, le nombre de Reynolds basé sur le diamètre hydraulique et les facteurs géométriques de l'espace annulaire. Les résultats expérimentaux, obtenus pour les écoulements tourbillonnaires laminaire et turbulent, sont corrélés à partir d'équations prenant en compte les paramètres mentionnés précédemment.

EINFLUSS DER EINTRITTSBEDINGUNGEN AUF DEN STOFFÜBERGANG IN EINER RINGSPALTSTRÖMUNG MIT ABKLINGENDER VERWIRBELUNG

Zusammenfassung—Mit Hilfe eines elektrochemischen Verfahrens werden die Stoffübergangskoeffizienten von einer Wand an eine Flüssigkeit experimentell untersucht, und zwar für den Fall einer verwirbelten Ringspaltströmung, die durch einen tangentialen Einlaß erzeugt wird. Besonderes Augenmerk wird auf den Einfluß des Verhältnisses aus Dicke e des Ringspaltes und Einlaßdurchmesser ϕ_e gelegt. Abhängig vom Wert dieses Verhältnisses ergeben sich drei unterschiedliche Strömungsformen: Die reine Wirbelströmung (für $\phi_e = e$), eine Strömung mit sich einengenden Wirbeln (für $\phi_e > e$) und eine Strömung mit sich aufweitenden Wirbeln ($\phi_e < e$). Darüberhinaus wird der Einfluß der folgenden Parameter untersucht: Der mittlere axiale Abstand der stoffübertragenden Oberflächen (zur Charakterisierung des Abklingens der Verwirbelung), die mit dem hydraulischen Durchmesser gebildete Reynolds-Zahl und die geometrischen Kennzahlen des Ringspalts. Abschließend werden die Versuchsdaten unter Berücksichtigung der erwähnten Parameter für laminare und turbulente Wirbelströmungen korreliert.

ВЛИЯНИЕ ВХОДНЫХ УСЛОВИЙ НА МАССОПЕРЕНОС В КОЛЬЦЕВОМ ЗАКРУЧЕННОМ ЗАТУХАЮЩЕМ ТЕЧЕНИИ

Аннотация—С использованием электрохимического метода экспериментально исследуются коэффициенты массопереноса от стенки к жидкости при кольцевом закрученном течении, образуемом тангенциальным входом. Основное внимание уделяется влиянию отношения толщины кольцевого канала e к диаметру входа ϕ_e. На основе значения данного отношения определены три режима течения: чисто закрученный поток при $\phi_e = e$, сужающийся закрученный поток при $\phi_e > e$ и расширяющийся закрученный поток для $\phi_e < e$. Другими исследуемыми параметрами являются среднее осевое расстояние между поверхностями теплообмена, которое используется для характеристики затухания закрутки, а также число Рейнольдса, основанное на гидравлическом диаметре и геометрических факторах кольцевого канала. Предложены соотношения для ламинарного и турбулентного закрученных течений, обобщающие экспериментальные данные с учетом вышеуказанных параметров.